

Enhanced space charge limited current for curved electron emitters

Gaurav Singh,^{1,2} Raghwendra Kumar,¹ and Debabrata Biswas^{1,2}

¹⁾*Bhabha Atomic Research Centre, Mumbai 400 085, INDIA*

²⁾*Homi Bhabha National Institute, Mumbai 400 094, INDIA*

The maximum current that can be transported across a vacuum diode is limited by the space charge force. In a planar diode configuration, the space charge limited (SCL) current density from a planar emitting patch is given by the Child-Langmuir (CL) law $J_{CL} \sim V_g^{3/2}/D^2$ where V_g is the potential difference across the diode and D is the separation between the anode and cathode. We show here analytically using the nonlinear line charge model that for a curved emitter in a planar diode configuration, the limiting current obeys the scaling relationship $J_{SCL} \sim \gamma_a V_g^{3/2}/D^2$ where γ_a is the apex field enhancement factor of the curved emitter. For an emitter with large height (h) to apex radius of curvature (R_a) ratio, the limiting current far exceeds the planar value. The result is verified using the particle-in-cell code PASUPAT for two curved emitters shapes.

I. INTRODUCTION

The maximum current that can be transported across a vacuum diode is a quantity of immense interest in vacuum microelectronics, space navigation and especially in high-power vacuum electronic devices such as magnetron, gyrotron, vircator or relativistic backward wave oscillators¹. The limit on the current arises from space charge forces which give rise to an electric field that opposes the macroscopic applied field in the diode. The current that enables an exact cancellation of these forces is referred to as the space charge limited (SCL) current. It is a quantity that can be reliably used to design systems and is used to model explosive emission in particle-in-cell (PIC) codes.

In a planar diode configuration, the SCL current density is given by the Child-Langmuir law^{2,3}

$$J_{CL} = \frac{4\epsilon_0}{9} \left(\frac{2e}{m} \right)^{1/2} \frac{V_g^{3/2}}{D^2} \quad (1)$$

where e and m are the electronic charge and mass respectively, V_g is the potential difference across anode-cathode gap and D refers to the distance between them. Eq. (1) strictly holds for a diode where the parallel plates are infinite in extent and the entire cathode participates in emission. Such a situation may approximate the case when the plate separation D is very small compared to the size of the emitting region. When they are comparable, a correction factor needs to be incorporated⁴⁻⁷

In recent decades, emission from curved surfaces under the application of an electric field has been extensively researched. A curved emitter placed perpendicular to the cathode plate in a planar diode configuration, has a local electric field at the apex which can be expressed as $E_a = \gamma_a E_0$ where $E_0 = V_g/D$ is the macroscopic field and $\gamma_a > 1$. This leads to larger field emission currents at moderate fields and can hasten explosive emission in high power systems. In such situations of emission from a curved surface, the space charge limited current is expected to increase and its exact nature is a matter of considerable interest. A clue that the scaling relationship $V_g^{3/2}/D^2$ should continue to hold for curved emitters, fol-

lows from the general scaling law for Schrödinger-Poisson system arrived at using dimensional analysis⁸ wherein $J \simeq \hbar^{3-2\alpha} V_g^\alpha / D^{5-2\alpha}$ where $\hbar = h/2\pi$, h being the Plank constant. For a purely classical system $3-2\alpha = 0$ so that $J \simeq V_g^{3/2}/D^2$ irrespective of the emitter shape⁹.

The limiting current is known analytically for co-axial cylindrical diodes and concentric spherical diode systems apart from the planar (Cartesian) system^{7,10-13}. A similar treatment for a curved emitter in a planar diode configuration seems beyond the scope of standard techniques and it is therefore necessary to take recourse to approximate analytical methods and PIC codes where space-charge limited emission from curved surfaces is modeled adequately. The aim of this work is to establish an extension of the Child-Langmuir law for curved emitters.

II. APPROXIMATE DERIVATION OF SCL CURRENT

The space charge limited current^{7,14} for zero injection velocity corresponds to the condition that the net electric field at the cathode is zero. We shall use approximate methods which incorporates this basic requirement and highlights the physical aspects. A simple derivation of the Child-Langmuir law based on vacuum capacitance and transit time^{7,15,16} provides much physical insight.

A. The Planar Case

Consider a planar diode with the anode and cathode separated by a distance D and having a potential difference V_g . The electric field between the plates is $E_0 = V_g/D$ and the induced surface charge density on the cathode plate is $\epsilon_0 E_0$. The total charge Q_b induced on an area \mathcal{A} is thus $Q_b = \epsilon_0 \mathcal{A} E_0 = \epsilon_0 \mathcal{A} V_g/D$. This is also the magnitude of the charge induced on the anode on an identical area \mathcal{A} since the field lines remain straight and perpendicular to the plates.

In order to address the question of space charge limited current, consider a charge filled flux tube having a cross-sectional area \mathcal{A} and extending from the cathode ($z = 0$) to the anode ($z = D$). Let the total charge

contained be Q such that the net field (the macroscopic field $-E_0\hat{z}$ and the space charge field) at the cathode is zero. It is assumed here that the field lines remain straight and perpendicular to the plates in the presence of the free charge Q (see Fig. 1). Consider, a Gaussian surface covering this tubular volume (dashed lines), with the faces parallel to the plates (marked 1 and 3) infinitesimally away from them. Since the net field at the cathode is zero, $\int_1 E \cdot dS = 0$ for the face (1) near the cathode. The flux through the transverse surface (labeled 2) is also zero while the flux through the surface near the anode is $E_0\mathcal{A}$ assuming that the field at the anode remains E_0 in the presence of the charge Q . In reality the field at the anode $E_A = \alpha_1 E_0$ with $\alpha_1 > 1$. Thus, the approximate total flux through the Gaussian surface is $\oint E \cdot dS = E_A\mathcal{A} \simeq E_0\mathcal{A} = \mathcal{A}V_g/D = Q/\epsilon_0$ so that the free charge $Q = \epsilon_0 E_0 \mathcal{A} = Q_b$ needs to reside in the diode in order that the field at the cathode is zero.

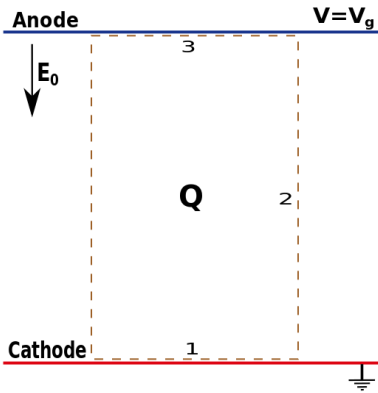


FIG. 1. A schematic of a planar diode and a Gaussian surface marked by dashed lines

Assuming now that the average transit time between the plates is $T_{av} = D/v_{av}$ where $v_{av} = v_{max}/2$ is the average speed and $v_{max} = (2eV_g/m)^{1/2}$ is the maximum speed, the space charge limited current through the diode is $I_{SCL} = Q/T_{av} = \mathcal{A}(\epsilon_0/2)(2e/m)^{1/2}V_g^{3/2}/D^2$. Note that in the actual planar 1-D situation, the average speed is $v_{av} = v_{max}/\alpha_2$ where $\alpha_2 = 3$ while $\alpha_1 = 4/3$. Thus $\alpha_1/\alpha_2 = 4/9$ as in the Child-Langmuir law of Eq. (1) instead of $1/2$. The approximate result is however close to the exact result and the derivation is considerably simpler.

B. SCL current for a curved emitter

We shall follow a similar procedure to determine the approximate SCL current for a curved emitter. In order to keep the derivation simple, we shall consider a hemi-ellipsoidal emitter of height h and apex radius of curvature R_a mounted on the cathode plane. As before, consider the diode without any free charge. Let the charge induced on the hemi-ellipsoidal emitter be Q_b . Consider a flux tube as a Gaussian surface as shown in Fig. 2a consisting of surfaces 1,2 and 3. Since surface 1 is inside

the hemi-ellipsoid, the flux through this is zero. Further, surface 2 is aligned along the field lines and hence the flux is again zero. The flux through surface 3 is $E_0\mathcal{A}_1$ where \mathcal{A}_1 is the cross-sectional area of the flux tube at the anode which is so far unknown. It follows from Gauss's law that $E_0\mathcal{A}_1 = Q_b/\epsilon_0$. Thus, $E_0\mathcal{A}_1$ can be determined if Q_b can be calculated.

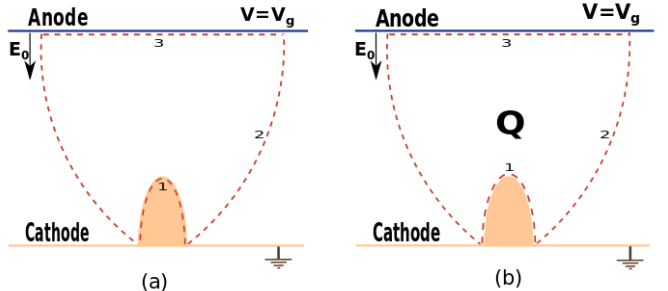


FIG. 2. A schematic of a planar diode with a hemi-ellipsoidal emitter along with Gaussian surfaces marked by dashed lines.

For a hemi-ellipsoid with the anode far away, the induced charge Q_b can be determined since the exact solution is known. It has also been established¹⁷ that the surface charge density can be projected on the axis as a line charge having linear density $\Lambda(z) = \lambda z$ where^{17,18} $\lambda \simeq 4\pi\epsilon_0 E_0/[\ln(4h/R_a) - 2]$ for h/R_a sufficiently large. The total bound charge therefore is $Q_b = \int_0^h \lambda z \, dz = \lambda h^2/2$. Combining the expressions for λ and Q_b , we have $Q_b = \lambda h^2/2 = \gamma_a \pi \epsilon_0 E_0 R_a h$ where¹⁸⁻²⁰ $\gamma_a \simeq (2h/R_a)/[\ln(4h/R_a) - 2]$ is the field enhancement factor at the apex of the hemi-ellipsoidal emitter (the local field at the apex is thus $E_0\gamma_a$). Thus $E_0\mathcal{A}_1 = \lambda h^2/2 = \gamma_a \pi E_0 b^2$ where we have used $hR_a = b^2$ where b is the radius of the hemiellipsoid base.

We are now in a position to deal with the space charge limited current. Consider the Gaussian surface shown in Fig. 2b containing free charge Q . In the SCL limit, the field on surface 1 is zero. We shall assume surfaces 2 and 3 to be identical to Fig. 2a. Thus, the flux through surface 2 is approximately zero while the flux through surface 3 is $E_0\mathcal{A}_1$. Using Gauss's law, the free charge $Q \simeq \epsilon_0 E_0 \mathcal{A}_1 \simeq \gamma_a \epsilon_0 \pi E_0 b^2$. Assuming as in the planar case that the average velocity $v_{av} = (2eV_g/m)^{1/2}/2$, the SCL current for a curved emitter is

$$I_{SCL} \simeq (\pi b^2) \gamma_a \frac{\epsilon_0}{2} \left(\frac{2e}{m} \right)^{1/2} \frac{V_g^{3/2}}{D^2}. \quad (2)$$

Compared to a planar emitter of area $\mathcal{A} = \pi b^2$, the SCL current for a curved emitter is greater by a factor γ_a .

As in the planar case, there are a number of approximations that may alter the factor 1/2. These include the field at the anode, the average transit time and finally the assumption that the \mathcal{A}_1 does not change in the presence of charges. The scaling $I_{SCL} \sim \gamma_a V_g^{3/2}/D^2$ should however be preserved despite these approximations.

An extension to a general axially symmetric curved emitter is somewhat non-trivial but can be similarly carried out by noting that the projected line charge density is in general nonlinear and has the form²⁰ $\Lambda(z) = zf(z)$. Thus,

$$Q_b = \int_0^h \Lambda(z) dz = f(h) \frac{h^2}{2} \left[1 - \int_0^h \frac{z^2 f'(z)}{h^2 f(h)} dz \right] \quad (3)$$

where²⁰ $f(h) = 4\pi\epsilon_0 E_0 \gamma_a R_a / 2h$. Thus, the total charge contained in the diode such that the field on cathode vanishes is $Q \simeq \epsilon_0 E_0 \mathcal{A}_1 = Q_b = f(h)(h^2/2)(1 - \mathcal{C}) = \gamma_a \pi E_0 R_a h (1 - \mathcal{C})$ where $\mathcal{C} = \int_0^h (z^2 f'(z)) / (h^2 f(h)) dz$ is a nonlinear correction factor that is a-priori unknown. Note that for a hemi-ellipsoid, $f'(z) = 0$ so that $\mathcal{C} = 0$.

Using the expression for average velocity as before, it follows that $I_{SCL} \simeq (\pi R_a h) \gamma_a (\epsilon_0/2) (2e/m)^{1/2} (1 - \mathcal{C}) V_g^{3/2} / D^2$. Thus, the linear dependence on the apex field enhancement factor γ_a is expected for other emitter shapes as well.

C. Incorporating Anode-Proximity and Shielding

The analysis so far has been for an isolated curved emitter. We shall now consider two competing effects that have been ignored so far, each of which affects the apex field enhancement factor. The presence of the anode in close proximity to the emitter-apex alters the line charge density. Thus the expression for λ no longer holds and it is necessary to include the effect of charges induced on the anode²¹. The net effect is an increase in local field at the emitter apex.

The presence of other emitters in close proximity also alters the local field at the apex due to electrostatic shielding^{22,23}. In such a situation, the local field decreases compared to its isolated value. Finally, the presence of other emitters coupled with the anode also contributes enormously^{24,25}. Fortunately, all of these effects can be incorporated approximately to express λ as²⁴ $\lambda \simeq 4\pi\epsilon_0 E_0 / [\ln(4h/R_a) - 2 - \alpha_A + \alpha_S - \alpha_{SA}]$ where α_A accounts for anode-proximity of an isolated emitter, α_S accounts for shielding due to all other emitters and α_{SA} is the indirect effect of other emitters mediated through the anode. The apex field enhancement factor thus takes the form $\gamma_a \simeq (2h/R_a) / [\ln(4h/R_a) - 2 - \alpha_A + \alpha_S - \alpha_{SA}]$ so that the relation $\lambda \simeq 4\pi\epsilon_0 E_0 \gamma_a R_a / 2h$ continues to hold. Similarly the expression for $f(h)$ applies for a nonlinear line-charge in the presence of other emitters and the anode. Thus, the central results for SCL current arrived at earlier in this section, continue to hold.

III. RESULTS FOR CURVED EMMITTERS USING PIC

A. Comparison with an existing result

In [26], the localized current density at the apex of a hyperboloid was reported to scale as $V_g^{3/2} / D^m$ with $m = 1.1 - 1.2$. This appears to be at variance with the results derived here and therefore needs scrutiny.

A diode in [26] consists of two hyperboloids, one of which is a plane at $z = 0$ acting as an anode and the other (cathode) with its apex located at $z = D$ having an apex radius of curvature R_a . The local field at the apex is $E_a = 2V_g/R_a / \ln(4D/R_a) = [(V_g/D)2D/R_a] / \ln(4D/R_a)$ for $D \gg R_a$ so that the enhancement factor can be expressed as $\gamma_a \simeq (2D/R_a) / \ln(4D/R_a)$.

The regime explored in [26] is $D \in [500 - 1000]\text{nm}$ with $R_a = 50\text{nm}$ and 100nm . For $R_a = 50\text{nm}$, the apex enhancement factor can be approximated by the fit $\gamma_a \simeq 0.952(D/R_a)^{0.754}$. Thus, the scaling $I_{SCL} \sim \gamma_a V_g^{3/2} / D^2 \sim V_g^{3/2} / D^{2-0.754} = V_g^{3/2} / D^{1.246}$. The exponent of D is close to the value of m observed in [26].

B. Comparison using the PIC code PASUPAT

In order to further validate the analytical findings reported here, we shall use a three dimensional fully electromagnetic relativistic PIC code²⁷ named PASUPAT developed by the authors. It uses the Yee grid based Finite Difference Time Domain Method to solve Maxwell's equations in electromagnetic solver module²⁸⁻³⁰. The code also has an electrostatic solver, which currently uses the multigrid method³¹ to solve Poisson equation. The charge-conserving current weighting scheme of Esirkepov³² is used to assign current densities to the grid points and the standard Boris method²⁷ is employed to move the charged particles. Apart from the Dirichlet and Neumann boundary conditions, a variety of open boundary conditions have been incorporated both in the electromagnetic and electrostatic³³ modules. For handling curved surfaces, the electromagnetic solver uses the Dey-Mitra algorithm^{34,35} while for the electrostatic solver, the discretization scheme in the cut-cell (computational cell lying partially inside two medium) has been modified to account for the reduced spacing between mesh points³⁶. For space-charge limited emission from curved surfaces, we have adapted the algorithms presented in [37] and [38]. The code uses VTK³⁹ library for writing files for visualization of simulation data. PASUPAT has been tested on standard benchmark problems. In the present context, it reproduces the Child-Langmuir law for planar diode, both for the finite and infinite emission area. We shall use it here to study the space charge limited current for curved emitters in a planar diode configuration.

We consider space charge limited emission from (a)

a hemi-ellipsoid emitter and (b) a hemi-ellipsoid on a cylindrical post (HECP). The anode, cathode and emitter are assumed to be perfect electric conductors. Periodic boundary condition imposed on the side walls of the simulation domain. Typical anode-cathode gap D was taken to be $15\mu\text{m}$ while the number of computational cells along direction of propagation of beam, N_z , was typically 256 or 512, while in the transverse direction N_x and N_y were taken to be 128. We have checked for convergence against N_x , N_y , N_z and time step Δt . The total number of macro-particles is typically 1.5×10^5 .

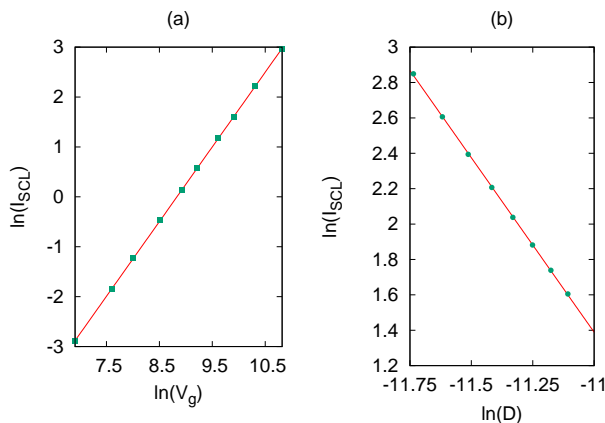


FIG. 3. Verification of scaling with V_g and D . Points are results obtained from simulation and line is best fit to the PIC simulation data. The emitter height $h = 3\mu\text{m}$. (a) The anode-cathode gap is held fixed at $D = 15\mu\text{m}$ while V_g is varied. Slope of the line is ≈ 1.49 (b) The voltage is held fixed at $V_g = 30\text{kV}$ while D is varied. The slope of the fitted line is ≈ 1.98 .

Fig. 3 shows the voltage scaling for an HECP emitter in a parallel plate diode configuration. The base radius $b = 1.5\mu\text{m}$, the height of the post is $1\mu\text{m}$ while the height of the hemiellipsoid-cap is $3\mu\text{m}$. We plot in Fig. 3a, $\ln(I_{SCL})$ against $\ln(V_g)$. Fitting a straight line yields a slope of 1.49 which is close to analytical prediction $I_{SCL} \sim V_g^{3/2}$. The scaling with anode-cathode plate gap D is shown in Fig. 3b (right panel) with $V_g = 3\text{kV}$. Fitting a straight line to the $\ln(I_{SCL})$ against $\ln(D)$ yields a slope of -1.98. These results further validate the voltage ($V_g^{3/2}$) and anode-cathode gap (D^{-2}) scaling for curved emitters arrived at analytically. A similar scaling has been found to hold for the hemi-ellipsoid emitter.

Finally, we present our study of variation of anode current with the apex field enhancement factor γ_a in Fig. 4. The left panel (Fig. 4a) shows the result for a hemiellipsoid. The enhancement factor is changed by varying the height of the hemiellipsoid while keeping the base radius fixed. The solid points are results obtained from PIC simulation while the straight line is best fit. It is clear that as predicted by our theory, anode current scales linearly with γ_a .

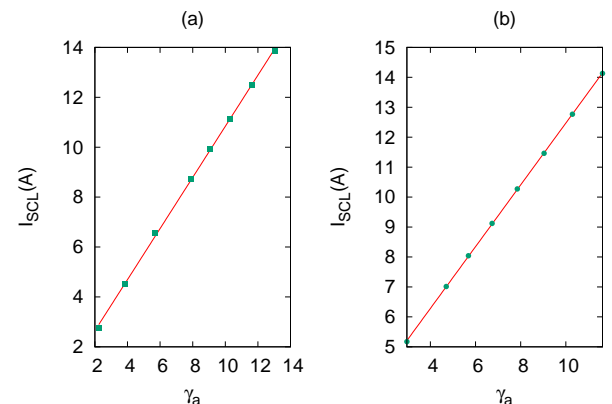


FIG. 4. Scaling of I_{SCL} with the apex enhancement factor γ_a for (a) hemiellipsoid (b) a hemiellipsoid endcap on cylindrical post. In both cases, the anode-cathode gap is $D = 15\mu\text{m}$ and the base radius of the emitter $b = 1.5\mu\text{m}$. The straight line is the best fit while the points are PIC simulation data. In (b) the height of the endcap is increased keeping the cylinder fixed.

We next consider an emitter having a hemi-ellipsoid end-cap mounted on top of a cylindrical post, a clear case of a nonlinear line charge density. As in the simulation study presented above, we change the height of emitter to change the apex field enhancement factor. The space charge limited current for different γ_a is plotted in the right panel (Fig. 4b). As before, solid points represent PASUPAT simulation data and line is best fit. It is evident again that the SCL current scales linearly with γ_a . We have tested these results for other geometries as well.

In conclusion, we have established that the space charge limited current for curved emitters obeys the scaling relationship $I_{SCL} \sim \gamma_a V_g^{3/2} / D^2$ which reduces to the Child-Langmuir law for $\gamma_a = 1$.

IV. REFERENCES

- ¹J. Benford, J. A. Swegle, and E. Schamiloglu, *High Power Microwaves*, Taylor & Francis Group, New York (2007).
- ²C. D. Child, Phys. Rev. 32, 492 (1911).
- ³I. Langmuir, Phys. Rev. 2, 450 (1913).
- ⁴J. W. Luginsland, Y. Y. Lau, and R. M. Gilgenbach, Phys. Rev. Lett. 77, 4668 (1996).
- ⁵Y. Y. Lau, Phys. Rev. Lett. 87, 278301 (2001).
- ⁶J. W. Luginsland, Y. Y. Lau, R. J. Umstatttd, and J. J. Watrous, Phys. Plasmas 9, 2371 (2002).
- ⁷P. Zhang, A. Valfells, L. K. Ang, J. W. Luginsland, and Y. Y. Lau, Appl. Phys. Rev. 4, 011304 (2017).
- ⁸D. Biswas and R. Kumar, EPL 102, 58002 (2013).
- ⁹For a diode with other length scales apart from D , the denominator can have quadratic combinations other than D^2 .
- ¹⁰I. Langmuir and K. B. Blodgett, Phys. Rev. 22, 347 (1923).
- ¹¹I. Langmuir and K. B. Blodgett, Phys. Rev. 24, 49 (1924).
- ¹²Y. B. Zhu, P. Zhang, A. Valfells, L. K. Ang, and Y. Y. Lau, Phys. Rev. Lett. 110, 265007 (2013).
- ¹³A. M. Darr and A. L. Garner, Appl. Phys. Lett. 115, 054101 (2019).

¹⁴R. R. Puri, D. Biswas, and R. Kumar, Phys. Plasmas 11, 1178 (2004).

¹⁵A. Rose, Phys. Rev. 97, 1538 (1955).

¹⁶R. J. Umstattd, C. G. Carr, C. L. Frenzen, J. W. Luginsland and Y. Y. Lau, American Journal of Physics 73, 160 (2005).

¹⁷D. Biswas, G. Singh, and R. Kumar, J. Appl. Phys. 120, 124307 (2016).

¹⁸E. G. Pogorelov, A. I. Zhabanov, and Y. C. Chang, Ultramicroscopy 109, 373 (2009).

¹⁹H. G. Kosmahl, IEEE Trans. Electron Devices 38, 1534 (1991).

²⁰D. Biswas, Phys. Plasmas 25, 043113 (2018).

²¹D. Biswas, Physics of Plasmas, 26, 073106 (2019).

²²D. Biswas and R. Rudra, Physics of Plasmas 25, 083105 (2018).

²³R. Rudra and D. Biswas, AIP Advances, 9, 125207 (2019).

²⁴D. Biswas and R. Rudra, J. Vac. Sci. Technol. B, J. Vac. Sci. Technol. B, 38, 023207 (2020).

²⁵D. Biswas, preprint, <https://arxiv.org/abs/2005.05700>

²⁶Y. B. Zhu and L. K. Ang, Physics of Plasmas, 22, 052106 (2015).

²⁷C K Birdsall and A. B. Langdon, "Plasma Physics via Computer Simulation", New York: McGraw-Hill, 1985.

²⁸K.S. Yee, IEEE Trans. Antennas Propagat., vol. AP-14, No. 3, pp. 302- 307, 1966.

²⁹A. Taflove and S. C. Hagness, "Computational Electrodynamics", second Edition, Artech House, Boston, 2000.

³⁰U. S. Innan and R. A. Marshal, "Numerical Electromagnetics: The FDTD Method", Cambridge University Press, Cambridge UK, 2011.

³¹W. L. Briggs, V. E. Henson, and S. F. McCormick, "A Multigrid Tutorial, 2nd Edition", SIAM, ISBN: 978-0-89871-462-3, (2000).

³²T. Zh. Esirkepov, Comput. Phys. Comm. 135, 144-153 (2001).

³³D. Biswas, G. Singh, and R. Kumar Physics of Plasmas 22, 093119 (2015).

³⁴S. Dey and R. Mittra, IEEE Microwave and Guided Wave Letters, VOL. 7, NO. 9, 1997.

³⁵S. Benkler, N. Chavannes and N. Kuster, IEEE Transactions on Antennas and Propagation, 54, 1843 (2006).

³⁶L. N. Dworsky, "Introduction to Numerical Electrostatics Using MATLAB" John Wiley & Sons, Inc. (2014)

³⁷J. J. Watrous, J. W. Luginsland, and G. E. Sasser, Physics of Plasmas 8, 289 (2001).

³⁸J. Loverich, C. Nieter, D. Smithe, S. Mahalingam, and P. Stoltz, "Charge conserving emission from conformal boundaries in electromagnetic PIC simulations", (2009) Available at <https://www.researchgate.net/profile/John.Loverich/publication/>

³⁹W. Schroeder et al. "The Visualization Toolkit", 3rd Edition. Kitware, Inc., 2003. Available at url: <http://www.vtk.org>.